Vol 17 No 7, July 2008
1674-1056/2008/17(07)/2466-12

Chinese Physics B

© 2008 Chin. Phys. Soc.
and IOP Publishing Ltd

# Radiation forces on a three-level atom in the high-order Bessel beams*

Wang Zheng-Ling(王正岭)[a)b)†] and Yin Jian-Ping(印建平)[b)‡]

[a)] *Department of Physics, Jiangsu University, Zhenjiang* 212013, *China*
[b)] *State Key Laboratory of Precision Spectroscopy, Department of Physics, East China Normal University, Shanghai* 200062, *China*

(Received 3 September 2007; revised manuscript received 2 March 2008)

The general expressions of the average dissipative and dipole forces acting on a Λ-configuration three-level atom in an arbitrary light field are derived by means of the optical Bloch equations based on the atomic density matrix elements, and the general properties of the average dissipative and dipole forces on a three-level atom in the linearly-polarized high-order Bessel beams (HBBs) are analysed. We find a resonant property (with two resonant peaks) of the dissipative force and a non-resonant property (with two pairs of non-resonant peaks) of the dipole force on the three-level atom, which are completely different from those on the two-level atom. Meanwhile we find a saturation effect of the average dissipative force in the HBB, which comes from the saturation of the upper-level population. Our study shows that the general expressions of the average dissipative and dipole forces on the three-level atom will be simplified to those of the two-level atom under the approximation of large detuning. Finally, we study the axial and azimuthal Doppler cooling of atoms in 1D optical molasses composed of two counter-propagating HBBs and discuss the azimuthal influence of the HBB on the Doppler cooling limit. We also find that the Doppler limit of atoms in the molasses HBB is slightly below the conventional Doppler limit of $\hbar\Gamma/(2k_{\rm B})$ due to the orbital angular momentum $l\hbar$ of the HBB.

**Keywords:** radiation forces, optical Bloch equations, three-level atom, azimuthal Doppler cooling
**PACC:** 3280, 3280P, 4250V, 4250

## 1. Introduction

It is well known that Bessel beam is a kind of non-diffraction one in free space, in which zeroth-order Bessel beam has a bright central maximum intensity, whereas high-order Bessel beams (HBBs) have a dark hollow central intensity and possess an angular momentum of $l\hbar$.[1] In 1987, Durnin *et al* [2] first experimentally generated a zeroth-order Bessel beam by illuminating an annular slit placed on the focal plane of a lens with a plane light wave. Later on, Herman *et al* [3] used a conically-shaped optical axicon to obtain a high-efficiency zero-order Bessel beam. In 1994, Lee *et al* [4] generated a first-order Bessel-like beam by using optical holographic technique. In 1996, Paterson and Smith[5] experimentally produced two high-order Bessel beams ($J_1$- and $J_{10}$-beam) from an illuminating Gaussian beam by using axicon-type computer-generated holograms. In 2000, Arlt and Dholakia[6] generated high-order Bessel beams with a high efficiency by illuminating an axicon with a Laguerre–Gaussian beam (LGB). On the other hand, theoretical studies on the interaction of a two-level atom with the hollow laser beam (HLB) possessing spin and orbital angular momentum, such as azimuthal Doppler shift in the HLB,[7] atomic motion in the HLB(s),[8] atomic dynamics in multiple LGBs,[9] Doppler cooling of ion cyclotron motion in counter-propagating LGBs,[10] radiation forces on a two-level atom in the one-dimensional (1D) molasses LGBs[11] and light-induced torque on moving atoms[12] and so on,[13] have become one of hot research subjects in atom and quantum optics. More recently, radiation pressure of a ladder configuration three-level atom in bichromatic travelling fields[14] and light-induced nonlinear effects[15] has been studied. However, to date the interaction of a three-level atom with a HLB possessing spin and orbital angular momentum, as well as the interaction of an atom with a high-order Bessel beam has not been studied.

*Project supported by the National Natural Science Foundation of China ( Grant Nos 10434060 and 10674047), the Natural Science Foundation of the Jiangsu Higher Institutions of China (Grant No 06KJB510020), and the Natural Science Foundation of Jiangsu University of China (Grant No 07JDG027).
†E-mail: zlwang@ujs.edu.cn
‡E-mail: jpyin@phy.ecnu.edu.cn

Generally, the laser frequency detuning $\delta$ from the atom resonant frequency is chosen as a few natural linewidths (several $\Gamma$) of neutral atoms in the Doppler laser cooling based on a two-level atomic model.[10,16] This cannot be used to well describe a real alkali metal atom with a hyperfine structure of ground states because the hyperfine splitting $\Delta_{\rm g}$ ($\sim$ a few GHzs) between the hyperfine ground states of alkali atoms is far larger than the laser detuning $\delta$ ($\sim$ a few MHzs) of Doppler cooling. In other words, only when the laser detuning $\delta$ is far larger than the ground-state hyperfine splitting $\Delta_{\rm g}$, a real alkali atom can be approximately described by a two-level atomic model. Therefore, a three-level atomic model is closer to the real case of laser cooling for real alkali atoms, and the interaction of a three-level atom with a light field (including a hollow laser beam) would be an interesting topic worthy to be studied.[17−20]

In this paper, we study the radiation forces on a three-level atom in the high-order Bessel beams and discuss the azimuthal Doppler cooling effect of the 1D molasses HBB. In Section 2, starting from the optical Bloch equations based on the atomic density matrix elements, we derive the expressions of the average dissipative and dipole forces acting on a Λ-configuration three-level atom in an arbitrary light field. In Section 3, we discuss the dependences of the average dissipative and dipole forces on the detuning (on the atomic velocity or on the radial position in the HBBs), and obtain the general properties of the dissipative and dipole forces on a three-level atom in the HBBs. In Section 4, we use two counter-propagating HBBs to form 1D optical molasses in both axial and azimuthal directions, and discuss the azimuthal influence of the HBB on the Doppler cooling limit. Some main results and conclusions are summarized in the last section.

## 2. The average dissipative and dipole forces on a three-level atom

We first consider the interaction of a Λ-configuration three-level atom with an arbitrary light field and then derive the general expressions of the average dissipative and dipole forces of light on the three-level atom in this section. As shown in Fig.1, the three-level atom is composed of an excited level $|3\rangle$ and two hyperfine ground levels$|1\rangle$, $|2\rangle$ with a hyperfine splitting of $\Delta_{\rm g}$. The atomic transition between $|1\rangle$ and$|3\rangle$, $|2\rangle$ and $|3\rangle$ are assumed to be optically allowed, while the transition between $|1\rangle$ and $|2\rangle$ is forbidden.

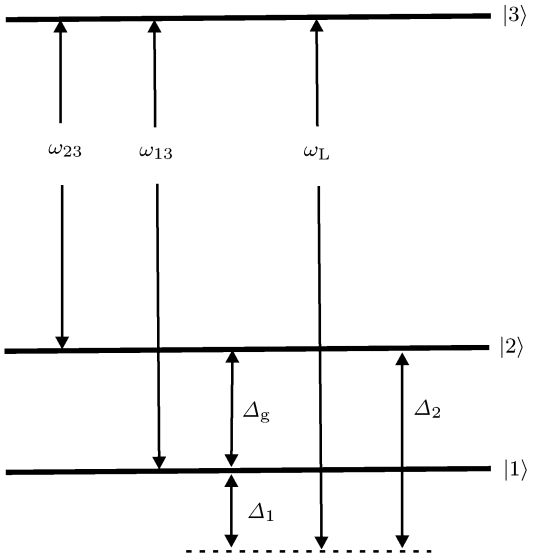



**Fig.1.** The Λ-configuration three-level atomic diagram.

In the electronic dipole and rotating wave approximations, the Hamiltonian of our atom–light interaction system can be written as

$$\begin{aligned} H =& \boldsymbol{P}^2/(2m) + U(\boldsymbol{R}) + \hbar\omega_1' |1\rangle\langle 1| + \hbar\omega_2' |2\rangle\langle 2| \\ &+ \hbar\omega_3' |3\rangle\langle 3| + \hbar\omega_{\rm L}\hat{a}^+\hat{a} + H_{\rm int}, \end{aligned} \tag{1}$$

where

$$\begin{aligned} H_{\rm int} =& -{\rm i}\hbar \left\{\hat{\pi}^+\hat{a}\, f_1(\boldsymbol{R}) - f_1^*(\boldsymbol{R})\, \hat{a}^+\pi\right\} \\ &- {\rm i}\hbar \left\{\hat{\sigma}^+\hat{a}\, f_2(\boldsymbol{R}) - f_2^*(\boldsymbol{R})\, \hat{a}^+\sigma\right\}. \end{aligned}$$

Here $\boldsymbol{P}$ and $\boldsymbol{R}$ are the momentum and position vectors of the atomic centre-of-mass with an atomic mass $m$, and $U(\boldsymbol{R})$ is the trapping potential for the atom. In Eq.(1), $\hbar\omega_1'$, $\hbar\omega_2'$ and $\hbar\omega_3'$ are the eigenenergies of the atomic levels $|1\rangle$, $|2\rangle$ and $|3\rangle$ respectively, and $\omega_{13} = \omega_3' - \omega_1'$, $\omega_{23} = \omega_3' - \omega_2'$ are the resonant transition frequencies of the atom, and $\omega_{\rm L}$ is the laser frequency and $\hat{a}^+(\hat{a})$ is the creation (annihilation) operator. The detuning of the laser frequency $\omega_{\rm L}$ from atomic transition $\omega_{13}(\omega_{23})$ is defined as $\Delta_1(\Delta_2)$. The symbols $\hat{\pi}^+$ and $\hat{\sigma}^+$ are the raising operators, and they represent the transitions from $|1\rangle$ to $|3\rangle$ and $|2\rangle$ to $|3\rangle$ respectively, while the transition operators $\hat{\pi}$ and $\hat{\sigma}$ are the lowering operators, and they represent the transitions from $|3\rangle$ to $|1\rangle$ and $|3\rangle$ to $|2\rangle$ respectively. $f_1(\boldsymbol{R})$ and $f_2(\mathbf{R})$ are two coupling parameters.

The last term $H_{\rm int}$ in Eq.(1) is the interaction Hamiltonian, which may be transformed to an inter-

action picture and given by

$$\begin{aligned} H'_{\rm int} =& -{\rm i}\hbar\ \left\{{\rm e}^{-{\rm i}\Delta_1 t}\ \pi^*\ a\ f_1\left(\boldsymbol{R}\right) - f_1^*\left(\boldsymbol{R}\right)\ a^*\ \pi\ {\rm e}^{{\rm i}\Delta_1 t}\right\} \\ & -{\rm i}\hbar\left\{{\rm e}^{-{\rm i}\Delta_2\, t}\ \sigma^*\ a\ f_2\left(\boldsymbol{R}\right)\right. \\ & \left. - f_2^*\left(\boldsymbol{R}\right)\ a^*\ \sigma\ {\rm e}^{{\rm i}\Delta_2\, t}\right\}, \end{aligned} \tag{2}$$

where the laser operators $\hat{a}^+$ and $\hat{a}$ have been replaced by $c$ numbers with[9]

$$\hat{a} = a{\rm e}^{-{\rm i}\omega_{\rm L} t}, \quad \hat{a}^+ = a^*{\rm e}^{{\rm i}\omega_{\rm L} t}. \tag{3}$$

Similarly, the transition operators $\hat{\pi}(\hat{\pi}^+)$ and $\hat{\sigma}(\hat{\sigma}^+)$ have been replaced by $c$ numbers with

$$\hat{\pi} = \pi{\rm e}^{-{\rm i}\,\omega_{13}\,t}, \quad \hat{\pi}^+ = \pi^*{\rm e}^{{\rm i}\,\omega_{13}\,t}, \tag{4a}$$

$$\hat{\sigma} = \sigma{\rm e}^{-{\rm i}\,\omega_{23}\,t}, \quad \hat{\sigma}^+ = \sigma^*{\rm e}^{{\rm i}\,\omega_{23}\,t}. \tag{4b}$$

The coupling parameters $f_1\left(\boldsymbol{R}\right)$ and $f_2\left(\boldsymbol{R}\right)$ can be written as respectively[9]

$$f_1\left(\boldsymbol{R}\right) = G_1\left(\boldsymbol{R}\right){\rm e}^{\,{\rm i}\theta(\boldsymbol{R})} \tag{5a}$$

and

$$f_2\left(\boldsymbol{R}\right) = G_2\left(\boldsymbol{R}\right){\rm e}^{\,{\rm i}\,\theta(\boldsymbol{R})}, \tag{5b}$$

where $G_1\left(\boldsymbol{R}\right) = \dfrac{1}{\hbar}\,\boldsymbol{D}_{13}\cdot\boldsymbol{\varepsilon}\left(\boldsymbol{R}\right)$ and $G_2\left(\boldsymbol{R}\right) = \dfrac{1}{\hbar}\,\mathbf{D}_{23}\cdot\boldsymbol{\varepsilon}\left(\boldsymbol{R}\right)$ correspond to two Rabi frequencies $\Omega_1$ and $\Omega_2$ respectively; $\boldsymbol{D}_{13}(\boldsymbol{D}_{23})$ is the dipole matrix element between the levels $|1\rangle$ ($|2\rangle$) and $|3\rangle$, and $\boldsymbol{\varepsilon}\left(\boldsymbol{R}\right)$ and $\theta\left(\boldsymbol{R}\right)$ are the amplitude and phase of the light field, respectively.

In order to derive the dissipative and dipole forces on a three-level atom in an arbitrary light field by using the optical Bloch equations based on the atomic density matrix elements, we take a semiclassical approximation and assume that the gross motion of the atom is classical while the internal dynamics of the atom is quantized. Therefore, the position and momentum operators $\boldsymbol{R}$ and $\boldsymbol{P}$ may be replaced by their expectation values $\boldsymbol{R}_0$ and $\boldsymbol{P}_0$, respectively. The atomic density matrix can be written as[9]

$$\rho = \delta\left(\boldsymbol{R}-\boldsymbol{R_0}\right)\delta\left(\boldsymbol{P}-\boldsymbol{P_0}\right)\rho\left(t\right), \tag{6a}$$

and the evolution of $\rho\left(t\right)$ is given by

$$\frac{{\rm d}\rho}{{\rm d}t} = -\frac{\rm i}{\hbar}\left[H,\rho\right] + \Re_\rho, \tag{6b}$$

where $\Re_\rho$ results from the relaxation dynamics of the three-level atomic system.

We find that the Hamiltonian in Eq.(1) can be transformed to an interaction picture and only the interaction Hamiltonian $H'_{\rm int}$ will not commute with $\rho\left(t\right)$. So using Eqs.(2) and (6b), the optical Bloch equations based on the density matrix elements can be written as

$$\begin{aligned} \frac{\rm d}{{\rm d}t}\tilde{\rho}_{33} =& -G_1\left(\boldsymbol{R_0}\right)\left({\rm e}^{{\rm i}[\theta(\boldsymbol{R_0})-\Delta_1 t]}a\tilde{\rho}_{13} + {\rm e}^{-{\rm i}[\theta(\boldsymbol{R_0})-\Delta_1 t]}a^*\tilde{\rho}_{31}\right) \\ & -G_2\left(\boldsymbol{R_0}\right)\left({\rm e}^{{\rm i}[\theta(\boldsymbol{R_0})-\Delta_2 t]}a\tilde{\rho}_{23} + {\rm e}^{-{\rm i}[\theta(\boldsymbol{R_0})-\Delta_2 t]}a^*\tilde{\rho}_{32}\right) - 2\left(\Gamma_1+\Gamma_2\right)\tilde{\rho}_{33}, \\ \frac{\rm d}{{\rm d}t}\tilde{\rho}_{22} =& G_2\left(\boldsymbol{R_0}\right)\left({\rm e}^{{\rm i}[\theta(\boldsymbol{R_0})-\Delta_2 t]}a\tilde{\rho}_{23} + {\rm e}^{-{\rm i}[\theta(\boldsymbol{R_0})-\Delta_2 t]}a^*\tilde{\rho}_{32}\right) + 2\Gamma_2\tilde{\rho}_{33}, \\ \frac{\rm d}{{\rm d}t}\tilde{\rho}_{11} =& G_1\left(\boldsymbol{R_0}\right)\left({\rm e}^{{\rm i}[\theta(\boldsymbol{R_0})-\Delta_1 t]}a\tilde{\rho}_{13} + {\rm e}^{-{\rm i}[\theta(\boldsymbol{R_0})-\Delta_1 t]}a^*\tilde{\rho}_{31}\right) + 2\Gamma_1\tilde{\rho}_{33}, \\ \frac{\rm d}{{\rm d}t}\tilde{\rho}_{31} =& -aG_1\left(\boldsymbol{R_0}\right){\rm e}^{{\rm i}[\theta(\boldsymbol{R_0})-\Delta_1 t]}\left(\tilde{\rho}_{11}-\tilde{\rho}_{33}\right) + {\rm i}aG_2\left(\boldsymbol{R_0}\right){\rm e}^{{\rm i}[\theta(\boldsymbol{R_0})-\Delta_2 t]}\tilde{\rho}_{21} - \left(\Gamma_1+\Gamma_2\right)\tilde{\rho}_{31}, \\ \frac{\rm d}{{\rm d}t}\tilde{\rho}_{32} =& -aG_2\left(\boldsymbol{R_0}\right){\rm e}^{{\rm i}[\theta(\boldsymbol{R_0})-\Delta_2 t]}\left(\tilde{\rho}_{22}-\tilde{\rho}_{33}\right) + {\rm i}aG_1\left(\boldsymbol{R_0}\right){\rm e}^{{\rm i}[\theta(\boldsymbol{R_0})-\Delta_1 t]}\tilde{\rho}_{12} - \left(\Gamma_1+\Gamma_2\right)\tilde{\rho}_{32}, \\ \frac{\rm d}{{\rm d}t}\tilde{\rho}_{12} =& -a^*G_1\left(\boldsymbol{R_0}\right){\rm e}^{-{\rm i}[\theta(\boldsymbol{R_0})-\Delta_1 t]}\tilde{\rho}_{32} - {\rm i}aG_2\left(\boldsymbol{R_0}\right){\rm e}^{{\rm i}[\theta(\boldsymbol{R_0})-\Delta_2 t]}\tilde{\rho}_{13}, \end{aligned} \tag{7}$$

where $\Gamma_1(\Gamma_2)$ is the spontaneous transition rate from level $|3\rangle$ to level $|1\rangle$ ($|2\rangle$). Because the typical value of $G_1$ (or $G_2$) is far smaller than the hyperfine splitting $\Delta_{\rm g} = |\Delta_1 - \Delta_2|$ (such as when $I < 10^8{\rm mW/cm^2}$, $G_1(G_2) < \Delta_{\rm g}/10$ for a $^{85}$Rb atom), the small coherence $\tilde{\rho}_{12}$ can be neglected in the following discussion. The average radiation force acting on the atom, relative to the average rate of the atomic-momentum

change, is defined as the minus average gradient of the interaction Hamiltonian[9]

$$\langle \boldsymbol{F} \rangle = -\langle \nabla H_{\mathrm{int}} \rangle = \langle \boldsymbol{F} \rangle_{\mathrm{diss}} + \langle \boldsymbol{F} \rangle_{\mathrm{dipo}}\,. \tag{8}$$

Substituting Eq.(2) into Eq.(8), and replacing $\boldsymbol{R}$ and $\boldsymbol{P}$ by their expectation values $\boldsymbol{R}_0$ and $\boldsymbol{P}_0$, the average dissipative and dipole forces can be written respectively by

$$\begin{aligned}\langle \boldsymbol{F} \rangle_{\mathrm{diss}} =& -\hbar\nabla\theta\left(\boldsymbol{R_0}\right)\{\tilde{\rho}_{13}\,\mathrm{e}^{\mathrm{i}[\theta(\boldsymbol{R_0})-\Delta_1 t]}aG_1\left(\boldsymbol{R_0}\right)+\tilde{\rho}_{31}\mathrm{e}^{-\mathrm{i}[\theta(\boldsymbol{R_0})-\Delta_1 t]}a^*G_1\left(\boldsymbol{R_0}\right)\\ &+\tilde{\rho}_{23}\mathrm{e}^{\mathrm{i}[\theta(\boldsymbol{R_0})-\Delta_2 t]}aG_2\left(\boldsymbol{R_0}\right)+\tilde{\rho}_{32}\mathrm{e}^{-i[\theta(\boldsymbol{R_0})-\Delta_2 t]}a^*G_2\left(\boldsymbol{R_0}\right)\},\end{aligned} \tag{9a}$$

$$\begin{aligned}\langle \boldsymbol{F} \rangle_{\mathrm{dipo}} =& \mathrm{i}\hbar\frac{\nabla G_1\left(\boldsymbol{R_0}\right)}{G_1\left(\boldsymbol{R_0}\right)}\{\tilde{\rho}_{13}\,\mathrm{e}^{\mathrm{i}[\theta(\boldsymbol{R_0})-\Delta_1 t]}aG_1\left(\boldsymbol{R_0}\right)-\tilde{\rho}_{31}\mathrm{e}^{-\mathrm{i}[\theta(\boldsymbol{R_0})-\Delta_1 t]}a^{\,*}G_1\left(\boldsymbol{R_0}\right)\}\\ &+\mathrm{i}\hbar\frac{\nabla G_2\left(\boldsymbol{R_0}\right)}{G_2\left(\boldsymbol{R_0}\right)}\{\tilde{\rho}_{23}\,\mathrm{e}^{\mathrm{i}[\theta(\boldsymbol{R_0})-\Delta_2 t]}aG_2\left(\boldsymbol{R_0}\right)-\tilde{\rho}_{32}\mathrm{e}^{-\mathrm{i}[\theta(\boldsymbol{R_0})-\Delta_2 t]}a^*G_2\left(\boldsymbol{R_0}\right)\}.\end{aligned} \tag{9b}$$

By using the following substitutions

$$\begin{aligned}\tilde{\rho}_{31} &= \tilde{\sigma}_{31}\mathrm{e}^{\mathrm{i}[\theta(\boldsymbol{R_0})-\Delta_1 t]},\\ \tilde{\rho}_{32} &= \tilde{\sigma}_{32}\mathrm{e}^{\mathrm{i}[\theta(\boldsymbol{R_0})-\Delta_2 t]},\end{aligned} \tag{10}$$

to eliminate the explicit time and position dependences in Eq.(7), we can simplify the density matrix equations as

$$\begin{aligned}\frac{\mathrm{d}}{\mathrm{d}t}\tilde{\rho}_{33} =& -G_1\left(a\tilde{\sigma}_{13}+a^*\tilde{\sigma}_{31}\right)-G_2\left(a\tilde{\sigma}_{23}+a^*\tilde{\sigma}_{32}\right)\\ &-2\left(\Gamma_1+\Gamma_2\right)\tilde{\rho}_{33},\\ \frac{\mathrm{d}}{\mathrm{d}t}\tilde{\rho}_{22} =& G_2\left(a\tilde{\sigma}_{23}+a^*\tilde{\sigma}_{32}\right)+2\Gamma_2\tilde{\rho}_{33},\\ \frac{\mathrm{d}}{\mathrm{d}t}\tilde{\rho}_{11} =& G_1\left(a\tilde{\sigma}_{13}+a^*\tilde{\sigma}_{31}\right)+2\Gamma_1\tilde{\rho}_{33},\\ \frac{\mathrm{d}}{\mathrm{d}t}\tilde{\sigma}_{31} =& -aG_1\left(\tilde{\rho}_{11}-\tilde{\rho}_{33}\right)+\left[\mathrm{i}\Delta_{\mathrm{T}1}-\left(\Gamma_1+\Gamma_2\right)\right]\tilde{\sigma}_{31},\\ \frac{\mathrm{d}}{\mathrm{d}t}\tilde{\sigma}_{32} =& -aG_2\left(\tilde{\rho}_{22}-\tilde{\rho}_{33}\right)\\ &+\left[\mathrm{i}\Delta_{\mathrm{T}2}-\left(\Gamma_1+\Gamma_2\right)\right]\tilde{\sigma}_{32}.\end{aligned} \tag{11}$$

From Eq.(10), the average dissipative and dipole forces can be rewritten respectively as

$$\begin{aligned}\langle \boldsymbol{F} \rangle_{\mathrm{diss}} =& -\hbar\nabla\theta\left\{\tilde{\sigma}_{13}\,aG_1+\tilde{\sigma}_{31}a^*G_1\right.\\ &\left.+\tilde{\sigma}_{23}aG_2+\tilde{\sigma}_{32}a^*G_2\right\},\end{aligned} \tag{12a}$$

$$\begin{aligned}\langle \boldsymbol{F} \rangle_{\mathrm{dipo}} =& \mathrm{i}\hbar\frac{\nabla G_1}{G_1}\ \{\tilde{\sigma}_{13}\,aG_1-\tilde{\sigma}_{31}a\,G_1\}\\ &+\mathrm{i}\hbar\frac{\nabla G_2}{G_2}\ \{\tilde{\sigma}_{23}\,aG_2-\tilde{\sigma}_{32}a\,G_2\}\,.\end{aligned} \tag{12b}$$

Substituting the steady-state solutions of Eqs.(11) into Eqs.(12), we derive the general expression of the average dissipative force for the three-level atom

$$\langle \boldsymbol{F} \rangle_{\mathrm{diss}} = 2\hbar\Gamma B\nabla\theta, \tag{13}$$

where

$$\begin{aligned}B =& \frac{\Gamma+\Gamma_2}{2\Gamma_1}\\ &\cdot\frac{\frac{-\Omega_1^2\Omega_2^2\left(\Gamma_1\Gamma+2\Gamma_1\Gamma_2+\Gamma_2\Gamma\right)}{\Gamma}+\left[\Gamma^2+\Delta_{\mathrm{T}2}^2+\left(1+\frac{\Gamma_2}{\Gamma}\right)\Omega_2^2\right]\Omega_1^2\Gamma_1+\left(\Gamma^2+\Delta_{\mathrm{T}1}^2+\left(1+\frac{\Gamma_1}{\Gamma}\right)\Omega_1^2\right)\Omega_2^2\Gamma_2}{\Gamma\left(\Gamma^2+\Delta_{\mathrm{T}1}^2+\left(1+\frac{\Gamma_1}{\Gamma}\right)\Omega_1^2\right)\left[\Gamma^2+\Delta_{\mathrm{T}2}^2+\left(1+\frac{\Gamma_2}{\Gamma}\right)\Omega_2^2\right]-\frac{\Omega_1^2\Omega_2^2\left(\Gamma+\Gamma_1\right)\left(\Gamma+\Gamma_2\right)}{\Gamma}},\end{aligned} \tag{14}$$

and the general expression of the average dipole force for the three-level atom is given by

$$\langle \boldsymbol{F} \rangle_{\rm dipo} = 2\hbar\nabla\Omega_1 \frac{\Delta_{\rm T1}\Omega_1\Omega_2^2\Gamma_2\left(\Gamma+\Gamma_1\right) - \left[\Gamma^2+\Delta_{\rm T2}^2+\left(1+\frac{\Gamma_2}{\Gamma}\right)\Omega_2^2\right]\Delta_{\rm T1}\Omega_1\Gamma_1\Gamma}{\Gamma^2\left(\Gamma^2+\Delta_{\rm T1}^2+\left(1+\frac{\Gamma_1}{\Gamma}\right)\Omega_1^2\right)\left[\Gamma^2+\Delta_{\rm T2}^2+\left(1+\frac{\Gamma_2}{\Gamma}\right)\Omega_2^2\right] - \Omega_1^2\Omega_2^2\left(\Gamma+\Gamma_1\right)\left(\Gamma+\Gamma_2\right)}$$
$$+ 2\hbar\nabla\Omega_2 \frac{\Delta_{\rm T2}\Omega_1^2\Omega_2\Gamma_1\left(\Gamma+\Gamma_2\right) - \left(\Gamma^2+\Delta_{\rm T1}^2+\left(1+\frac{\Gamma_1}{\Gamma}\right)\Omega_1^2\right)\Delta_{\rm T2}\Omega_2\Gamma_2\Gamma}{\Gamma^2\left(\Gamma^2+\Delta_{\rm T1}^2+\left(1+\frac{\Gamma_1}{\Gamma}\right)\Omega_1^2\right)\left[\Gamma^2+\Delta_{\rm T2}^2+\left(1+\frac{\Gamma_2}{\Gamma}\right)\Omega_2^2\right] - \Omega_1^2\Omega_2^2\left(\Gamma+\Gamma_1\right)\left(\Gamma+\Gamma_2\right)}, \tag{15}$$

where $\Omega_1 = a\,G_1(\boldsymbol{R})$ and $\Omega_2 = a\,G_2(\boldsymbol{R})$ are two position dependent Rabi frequencies, and $\Delta_{\rm T1} = \Delta_1 - \nabla\theta(\boldsymbol{R})\cdot\boldsymbol{v}$ and $\Delta_{\rm T2} = \Delta_2 - \nabla\theta(\boldsymbol{R})\cdot\boldsymbol{v}$ are two effective detuning frequencies. Here $-\nabla\theta(\boldsymbol{R})\cdot\boldsymbol{v}$ is the Doppler frequency shift, and $\Gamma$ is the spontaneous transition rate of the excited level $|3\rangle$.

Only when the small velocity regime, where $|\nabla\theta\cdot\boldsymbol{v}| < \Gamma$ is considered, Eq.(13) can be expanded and taken to the first-order approximation in velocity, and the dissipative force on the atom can be written as a sum of a velocity–independent force and a velocity–dependent force, that is,

$$\langle \boldsymbol{F} \rangle_{\rm diss} \approx \langle \boldsymbol{F}_0 \rangle_{\rm diss} + \langle \boldsymbol{F}_{\boldsymbol{v}} \rangle_{\rm diss}, \tag{16}$$

where

$$\langle \boldsymbol{F}_0 \rangle_{\rm diss} = \frac{M}{P} 2\hbar\Gamma\nabla\theta, \tag{17a}$$

$$\langle \boldsymbol{F}_{\boldsymbol{v}} \rangle_{\rm diss} = \left(\frac{QM}{P^2} - \frac{N}{P}\right) 2\hbar\Gamma\nabla\theta\,(\nabla\theta\cdot\boldsymbol{v}), \tag{17b}$$

and

$$M = \frac{\left(\Gamma+\Gamma_2\right)\Gamma^2\Omega_1^2}{2} + \frac{\left(\Gamma+\Gamma_2\right)\Delta_2^2\Omega_1^2}{2} + \frac{\left(\Gamma+\Gamma_2\right)\Gamma_2\Delta_1^2\Omega_2^2}{2\Gamma_1} + \frac{\left(\Gamma+\Gamma_2\right)\Gamma^2\Gamma_2\Omega_2^2}{2\Gamma_1}, \tag{18a}$$

$$N = \frac{\left(\Gamma+\Gamma_2\right)\Gamma_2\Delta_1\Omega_2^2}{\Gamma_1} + \left(\Gamma+\Gamma_2\right)\Delta_2\Omega_1^2, \tag{18b}$$

$$P = \Gamma^5 + \left(\Gamma+\Gamma_2\right)\Gamma^2\Omega_2^2 + \left(\Gamma+\Gamma_1\right)\Gamma^2\Omega_1^2 + \Gamma^3\Delta_1^2 + \Gamma^3\Delta_2^2 + \Gamma\Delta_1^2\Delta_2^2, \tag{18c}$$

$$Q = 2\Gamma^3\Delta_1 + 2\Gamma^3\Delta_2 + 2\Gamma\Delta_1^2\Delta_2 + 2\Gamma\Delta_1\Delta_2^2. \tag{18d}$$

Moreover, under the approximation of large detuning, that is $|\Delta_1| >> \Delta_{\rm g}$, the average dissipative force of a three-level atom as shown by Eq.(13) can be approximate to

$$\langle \boldsymbol{F} \rangle'_{\rm diss} \approx 2\hbar \frac{\Omega_1^2\Gamma\nabla\theta}{\left(\Delta_1 - \nabla\theta\cdot\boldsymbol{v}\right)^2 + 2\Omega_1^2 + \Gamma^2}, \tag{19}$$

which is the same as the result of a two-level atom in the HLB.[9,10]

Similarly, when $|\Delta_1| >> \Delta_{\rm g}$, the average dipole force of a three-level atom as shown by Eq.(15) can be approximately reduced to

$$\langle \boldsymbol{F} \rangle'_{\rm dipo} = -\frac{2\hbar\left(\Delta_1 - \nabla\theta\cdot\boldsymbol{v}\right)\Omega_1\nabla\Omega_1}{\left(\Delta_1 - \nabla\theta\cdot\boldsymbol{v}\right)^2 + 2\Omega_1^2 + \Gamma^2}, \tag{20}$$

which is also the same as the result of a two level atom in the HLB.[9]

## 3. The properties of the average dissipative and dipole forces in linearly-polarized HBBs

A high-order Bessel beam is a diffraction-free and hollow laser beam, and the electric field amplitude of a linearly-polarized $l$th-order Bessel beam travelling along the $z$ direction can be expressed as[1]

$$E_l(r,\phi,z) = [A/w(z)]\exp(\mathrm{i}k_z z)J_l(k_r r) \times \exp(\mathrm{i}l\phi), \tag{21}$$

where $A$ is a normalization constant, $k_r$ and $k_z$ are the radial and axial components of the wavevector $k$ and $k = 2\pi n/\lambda = \sqrt{k_z^2 + k_r^2}$(here $k_r \le 0.01k$[6] and we can take $k_z = k$), $J_l$ is the $l$th-order Bessel beam with an integer $l$, which characterizes the quantum number of the orbital angular momentum, and $w^2(z) = 2\left(z_{\rm R}^2 + z^2\right)/(kz_{\rm R})$ is the beam width at the propagation distance $z$ from the beam waist with a Rayleigh length of $z_{\rm R}$. From Eq.(21), the phase $\theta(\boldsymbol{R})$ of the light field can be expressed as

$$\theta(\boldsymbol{R}) = k_z z + l\phi. \tag{22}$$

Therefore, the expression of $\nabla\theta(\boldsymbol{R})$ can be given by

$$\nabla\theta(\boldsymbol{R}) = k_z\hat{\boldsymbol{z}} + \frac{l}{r}\hat{\phi}, \tag{23}$$

where $\hat{z}$ and $\hat{\phi}$ are the axial and azimuthal unit vectors in the HBB, respectively. From Eq.(23), we find that the Doppler frequency shift $-\nabla\theta(\boldsymbol{R})\cdot\boldsymbol{v}$ is $-k_z v_z - \frac{l}{r}v_\phi$. Here $-k_z v_z$ is the axial Doppler frequency shift, which is the same as the result from the plane wave approximation and is larger (or smaller) than zero as $\nu_z < 0$ (or $\nu_z > 0$); whereas $-\frac{l}{r}v_\phi$ is the azimuthal Doppler frequency shift, which is the same as the result from the LGB[7] and is larger (or smaller) than zero as $v_\phi < 0$ (or $v_z > 0$).

The average dissipative force on the three-level atom in a linearly-polarized HBB can be derived by substituting Eq.(23) into Eq.(13), and is given by

$$\langle \boldsymbol{F}\rangle_{\rm diss} = \langle \boldsymbol{F}_{\rm axia}\rangle_{\rm diss} + \langle \boldsymbol{F}_{\rm azim}\rangle_{\rm diss}\,. \tag{24}$$

The first term in Eq.(24) is the axial component of the average dissipative force and can be given by

$$\langle \boldsymbol{F}_{\rm axia}\rangle_{\rm diss} = 2\hbar\Gamma B k_z \hat{\boldsymbol{z}}, \tag{25}$$

which results from the axial mode of the HBB and is a dominant component of the average dissipative force.

The second term in Eq.(24) is the azimuthal component of the average dissipative force and can be written as

$$\langle \boldsymbol{F}_{\rm azim}\rangle_{\rm diss} = 2\hbar\Gamma B\frac{l}{r}\hat{\phi}, \tag{26}$$

which is proportional to $l/r$ and acts on the azimuthal direction of atomic motion. In Eqs.(25) and (26), $B$ is given by Eq.(14). From Eq.(26), obviously, we can derive a torque on the atom along the beam axis, which is given by $\langle \boldsymbol{T}\rangle = 2\hbar\Gamma B l\hat{\boldsymbol{z}}$. Similarly, the dipole force and the approximate expressions of the average dissipative and dipole forces on an atom in a HBB can also be derived by substituting Eq.(23) into Eqs.(15), (16), (19) and (20) respectively.

## 3.1. The average azimuthal dissipative force

The azimuthal component $2\hbar\Gamma Bl/r$ of the average dissipative force (see Eq.(26)) on an atom in a HBB is proportional to the orbital angular-momentum quantum number $l$ and inversely proportional to the radial position $r$ of atomic motion in the HBB, by which the atom will be rotated in the azimuthal direction. For a three-level $^{85}$Rb atom in a linearly-polarized HBB, the $|1\rangle$ state corresponds to a $5S_{1/2}$, $F$=2 state, the $|2\rangle$ state corresponds to a $5S_{1/2}$, $F$=3 state, the $|3\rangle$ state corresponds to a $5P_{3/2}$ state, and $\Delta_{\rm g}/(2\pi) = 3.0\,{\rm GHz}$, $\lambda = 0.78\,\mu{\rm m}$, $\Gamma/(2\pi) = 6.0\,{\rm MHz}$, $\Gamma_1 = 0.74\Gamma$, $\Gamma_2 = 0.26\Gamma$, $\Omega_1 = \Omega_2 = 2\sqrt{I/(2I_{\rm sat})}\Gamma/3$, $I_{\rm sat}$=1.6mW/cm$^2$. From Eqs.(26) and (19), taking $l/r$=0.1$k$ and $I$=0.8mW/cm$^2$, that is, for the on-resonance saturation parameter $s_0 = I/I_{\rm sat}$=0.5, we calculate the dependence of the average azimuthal dissipative force on the detuning $\Delta_1/(2\pi)$, and the result is shown in Fig.2. We know from Fig.2 that there are two maximum average azimuthal dissipative forces appearing at the detuning $\Delta_1/(2\pi) = 0$ and $\Delta_1/(2\pi) = -\Delta_{\rm g}/(2\pi)$ for $\nabla\theta(\boldsymbol{R})\cdot\boldsymbol{v} = 0$GHz, which shows a resonant property (with two resonant peaks) of the azimuthal dissipative force on the three-level atom and comes from two resonant effects between $|1\rangle \to |3\rangle$ and between $|2\rangle \to |3\rangle$. It is clear that the resonant property of the average azimuthal dissipative force on the three-level atom is completely different from that on the two-level atom, which has only one resonant peak at $\Delta_1/(2\pi) = 0$ or $\Delta_1/(2\pi) = -\Delta_{\rm g}/(2\pi)$. We also find from Fig.2 that the positions of the two maximum average azimuthal dissipative forces will be shifted by an amount $\nabla\theta(\boldsymbol{R})\cdot\boldsymbol{v}$ (as shown by the dashed line in Fig.2 where $\nabla\theta(\boldsymbol{R})\cdot\boldsymbol{v} = 0.04$GHz corresponding to $v_z \sim$30m/s) to the right for $\nabla\theta(\boldsymbol{R})\cdot\boldsymbol{v} > 0$ or shifted to the left for $\nabla\theta(\boldsymbol{R})\cdot\boldsymbol{v} < 0$ due to Doppler frequency shift. In Fig.2, the dotted line is the average azimuthal dissipative force from the two-level atomic model, calculated using Eq.(19), and its maximum value and full width at half maximum (FWHM) value are $2.5\times10^{-2}\hbar k\Gamma$ and 0.015GHz respectively, which are larger than those ($1.7\times10^{-2}\hbar k\Gamma$ and 0.012GHz) from the three-level atomic model. This shows that the resulting error in calculation of the maximum azimuthal dissipative force at the resonant position $\Delta_1/(2\pi) = 0$ and its FWHM are respectively 47% and 25% if the two-level atomic model is used. We also find from Fig.2 that when the light frequency is tuned away from two resonant peaks, the average azimuthal dissipative force will be rapidly decreased. However, the average azimuthal dissipative force (see Eq.(19)) from the two-level atomic model will be equal to that shown by Eq.(26) when the detuning from the resonant peak is larger than $\sim$0.03GHz. In this case, the average dissipative-force expression $\langle \boldsymbol{F}\rangle_{\rm diss}$ (see Eq.(13)) from the three-level atomic model can be approximated by the expression $\langle \boldsymbol{F}\rangle'_{\rm diss}$ (see Eq.(19)) from the two-level atomic model.

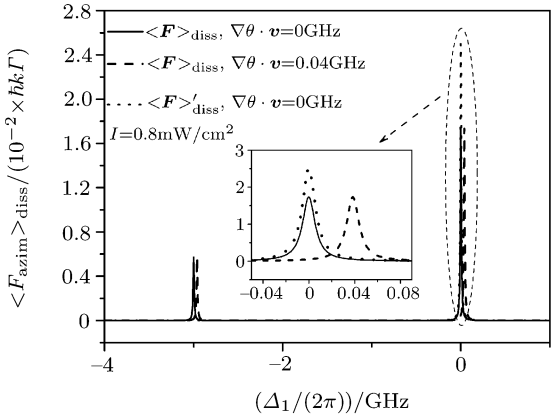



**Fig.2.** The dependence of the average azimuthal dissipative force component by using Eq.(26) as $\nabla\theta\,(\boldsymbol{R})\cdot\boldsymbol{v}=0$GHz (solid line) and $\nabla\theta\,(\boldsymbol{R})\cdot\boldsymbol{v}=0.04$GHz (dashed line) on $\Delta_1/(2\pi)$ for a $^{85}$Rb atom as $I$=0.8mW/cm$^2$. The dotted line stands for the average azimuthal dissipative force by using Eq.(19) as $\nabla\theta\,(\boldsymbol{R})\cdot\boldsymbol{v}=0$GHz.

In the small velocity regime where $|\nabla\theta\cdot\boldsymbol{v}|<\Gamma$, by substituting Eq.(23) into Eq.(17), we can derive the velocity-independent and the velocity-dependent average dissipative forces, which are given by

$$\langle\boldsymbol{F}_0\rangle_{\rm diss}=\frac{2\hbar\Gamma M}{P}\left(k_z\hat{\boldsymbol{z}}+\frac{l}{r}\hat{\boldsymbol{\varphi}}\right), \tag{27a}$$

$$\langle\boldsymbol{F}_v\rangle_{\rm diss}=2\hbar\Gamma\left(\frac{QM}{P^2}-\frac{N}{P}\right)\left[\left(k_z^2v_z+\frac{lk_z}{r}v_\phi\right)\hat{\boldsymbol{z}}+\left(\frac{lk_zv_z}{r}+\frac{l^2}{r^2}v_\phi\right)\hat{\boldsymbol{\phi}}\right], \tag{27b}$$

where $M,N,P$ and $Q$ are given by Eq.(18). Equation (27a) is the static (velocity-independent) average dissipative force, in which $2\hbar\Gamma Mk_z/P$ is the axial component acting on the atom along the light propagation and related to the photon momentum and the laser detuning, while $2\hbar\Gamma Ml/Pr$ is the azimuthal component is proportional to $l/r$ and can result in the rotation of atoms in the HBB. Equation (27b) is the velocity-dependent average dissipative force which includes its axial and azimuthal components, and is far smaller than the static average dissipative force in the small velocity regime, but it can be used to slow down the azimuthal motion of atoms in a HBB.

If a three-level atom moves in the two counter-propagating HBBs (i.e., 1D molasses HBBs) with two mutually-perpendicular linear polarizations (in order to eliminate the interference between the two laser beams) and the same frequency, amplitude, wave vector (i.e., $|k_1|=|k_2|$) and the quantum number of the orbital angular-momentum (i.e., $l_1=l_2=l$), it will experience a velocity-independent and a velocity-dependent average dissipative forces, which can be written as

$$\langle\boldsymbol{F}_0\rangle_{\rm diss}=0, \tag{28a}$$

$$\langle\boldsymbol{F}_v\rangle_{\rm diss}=-\beta_{\rm axia}v_z\hat{\boldsymbol{z}}-\beta_{\rm azim}v_\phi\hat{\boldsymbol{\phi}}, \tag{28b}$$

where

$$\beta_{\rm axia}=-4\hbar\Gamma\left(\frac{QM}{P^2}-\frac{N}{P}\right)k_z^2 \tag{29a}$$

and

$$\beta_{\rm azim}=-4\hbar\Gamma\left(\frac{QM}{P^2}-\frac{N}{P}\right)\frac{l^2}{r^2} \tag{29b}$$

are the two friction coefficients in the axial and azimuthal directions, respectively. If we use the expression of the average dissipative force (see Eq.(19)) to calculate the two friction coefficients, we can obtain

$$\beta'_{\rm axia}=-\frac{8\hbar\Omega_1^2\Gamma\Delta_1}{\left(\Delta_1^2+2\Omega_1^2+\Gamma^2\right)^2}k_z^2 \tag{30a}$$

and

$$\beta'_{\rm azim}=-\frac{8\hbar\Omega_1^2\Gamma\Delta_1}{\left(\Delta_1^2+2\Omega_1^2+\Gamma^2\right)^2}\frac{l^2}{r^2}. \tag{30b}$$

We know from Eq.(28) that there is no a static (velocity-independent) average dissipative force on the atoms in 1D molasses HBBs and the axial (or azimuthal) velocity-dependent force is called a velocity-dependent friction force which can be used to slow down the axial (or azimuthal) velocity of atomic motion and realize the axial (or azimuthal) Doppler cooling for $\beta_{\rm axia}>0$ (or $\beta_{\rm azim}>0$). From Eq.(29b), we calculate the dependence of the azimuthal friction coefficient $\beta_{\rm azim}$ on the detuning for $I$=0.8mW/cm$^2$ and $l/r$=0.1$k$, and the result is shown in Fig.3. We can see from Fig.3 that when the laser frequency is red detuned from the resonant frequency $\Delta_1/(2\pi)=0$ (or $-\Delta_{\rm g}/(2\pi)$), the azimuthal friction coefficient $\beta_{\rm azim}$ is larger than zero and the maximum $\beta_{\rm azim}$ value appears, at the detuning of $\sim-\Gamma/(4\pi)$ from the resonant frequency, which can be used to slow down the atomic motion. When the laser detuning relative to the resonant frequency is blue one, the coefficient $\beta_{\rm azim}$ is smaller than zero, which will result in the acceleration of atomic motion. We can also find from Fig.3 that the azimuthal friction coefficient (see Eq.(30b)) calculated from the two-level atomic model, as shown by the dotted line, is larger than that (see Eq.(29b)) from the three-level model, and the maximum relative error can be reached 29%; but it will be equal to that from the three-level model as the detuning from the resonant frequency is larger than ∼0.03GHz. In this case, the friction coefficient from the three-level atomic model can be approximated by the expression from the two-level atomic model. In

addition, the axial friction coefficient $\beta_{\rm axia}$ has a similar dependence on the detuning.

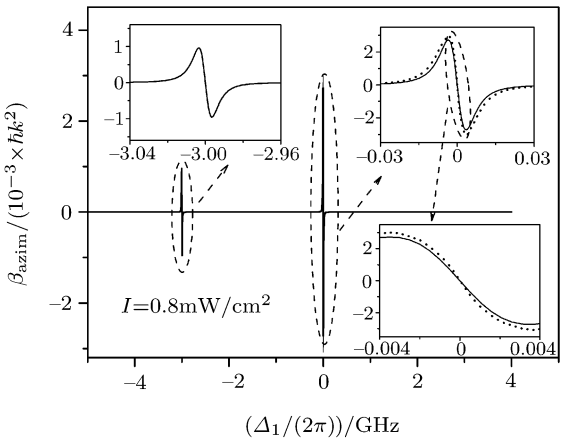



**Fig.3.** The dependence of the azimuthal friction coefficient (using Eq.(29b) (solid line) and using Eq.(30b) (dotted line)) on $\Delta_1/(2\pi)$ for a $^{85}$Rb atom for $I$=0.8mW/cm$^2$ and $l/r$=0.1$k$.

From Eqs.(26), (19) and (28b), for $I$=0.8mW/cm$^2$, $v_z$=0, $l/r$=0.1$k$ and $\Delta_1 = -\Gamma$, we have calculated the dependence of the average azimuthal dissipative force acting on a three-level $^{85}$Rb atom on the atomic velocity $v_\phi$, and the result is shown in Fig.4. The dashed line in Fig.4 corresponds to the average azimuthal dissipative force (see Eq.(26)) on a three-level $^{85}$Rb atom, which comes from a HBB propagating along the $z$ direction, and the dotted line corresponds to that coming from another HBB propagating in the $-z$ direction, while the solid line corresponds to the total average azimuthal dissipative force on a three-level $^{85}$Rb atom from the two counter-propagating HBBs, the dot-dashed line corresponds to the approximate expression of the velocity-dependent azimuthal linear friction force given by Eq.(28b), and the double-dot-dashed line corresponds to the total average azimuthal dissipative force (see Eq.(19)) from the two-level atomic model. It can be seen from Fig.4 that two counter-propagating HBBs form a 1D optical molasses in the azimuthal direction and produce a pure damping force on the atoms in a 2D (or 3D) ring optical dipole trap within the small velocity regime for $\Delta_1 < 0$. It can also be seen from Fig.4 that the average azimuthal dissipative force based on the three-level atomic model is lower than that based on the two-level atomic model and the maximum relative error can reach 42% when the azimuthal velocity is less than $0.5\Gamma/k$ ($\sim$ 2.3m / s) for $I$=0.8mW/cm$^2$, $v_z$=0, $l/r$=0.1$k$ and $\Delta_1 = -\Gamma$. Figures 3 and 4 show that if the two-level atomic model is used to calculate the average azimuthal dissipative force and its friction coefficient for a real alkali atom, the resulting errors are considerable.

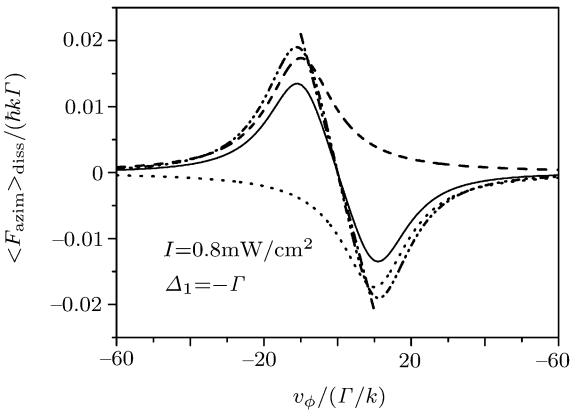



**Fig.4.** The dependence of the average azimuthal dissipative force on the atomic velocity $v_\phi$ for a $^{85}$Rb atom for $I$=0.8mW/cm$^2$, $v_z$=0, $l/r$=0.1$k$ and $\Delta_1 = -\Gamma$. The dashed (dotted) line stands for the average azimuthal dissipative force by applying Eq.(26) to a three-level $^{85}$Rb atom from one HBB propagating along the $z$ ($-z$) direction, while the solid line is calculated using Eq.(26) from the two counter-propagating HBBs, the dot-dashed line is calculated using Eq.(28b), and the double-dot-dashed-line is calculated using Eq.(19).

Furthermore, the dependence of the average azimuthal dissipative force on the radial position $r$ in a HBB is also studied, and the results are shown in Fig.5. In our calculation, the HBB parameters used are $P$=10 mW, $k_r$=0.01$k$, $l$=1, $\Delta_1/(2\pi) = 20\Gamma/(2\pi)$, $10\Gamma/(2\pi)$ and $1\Gamma/(2\pi)$. We find from Fig.5 that the radial distribution of the average azimuthal dissipative force is similar to the intensity profile of the HBB in the case of large detuning and small intensity, whereas the distribution of the average azimuthal dissipative force is distorted, relative to the intensity profile of the HBB for a small detuning or a large intensity. In particular, when the beam intensity is high and the detuning is small (such as when $\Delta_1/(2\pi) \leq 1\Gamma/(2\pi)$, $I \geq 5\times10^3$mW/cm$^2$), the saturation phenomenon of the average azimuthal dissipative force will appear. For the same intensity, the smaller the detuning is, the greater the saturation effect will be, while for the same detuning, the higher the intensity is, the greater the saturation effect will be. It is clear that the saturation phenomenon of the average azimuthal dissipative force results from the saturation effect of the spontaneous emission (that is, the saturation effect of the upper-level population in Eq.(14)) of the three-level atom in the HBB.

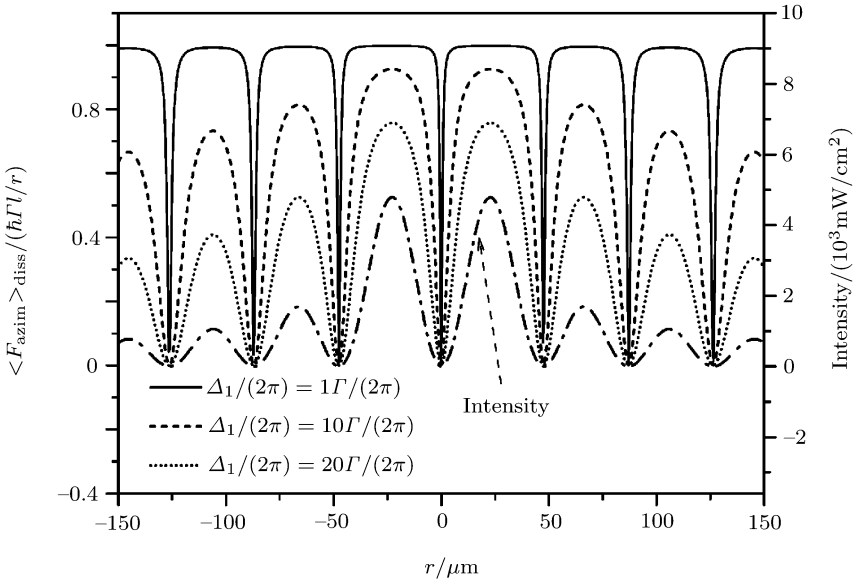



**Fig.5.** The dependence of the average azimuthal dissipative force component on the radial position $r$ in a HBB for a $^{85}$Rb atom for $P$=10 mW, $k_r$=0.01$k$, $l$=1, $\Delta_1/(2\pi) = 20\Gamma/(2\pi)$, $10\Gamma/(2\pi)$ and $1\Gamma/(2\pi)$.

## 3.2. The average axial dissipative force

The axial component of the average dissipative force from the HBB, as shown in Eq.(25), is the same as the result from the plane wave propagating along the $z$ axis with a wavevector of $k_z$. It is clear from Eq.(25) that similar to the azimuthal dissipative force, there are two maximum average axial dissipative forces, which appear at the detuning $\Delta_1/(2\pi) = 0$ and $\Delta_1/(2\pi) = -\Delta_{\rm g}/(2\pi)$ for $\nabla\theta\,(\boldsymbol{R})\cdot\boldsymbol{v} = 0$.

In the approximation of the small velocity, the average axial dissipative force on the three-level atom can be expressed as a sum of a velocity-independent and a velocity-dependent components. In Eq.(27), the velocity-independent average axial dissipative force is not related to the sign of the detuning. If two counter-propagating HBBs have the same parameters, the static (velocity-independent) average axial dissipative force will disappear, as shown in Eq.(28a); meanwhile the atoms will suffer a velocity-dependent average axial friction force, as shown in Eq.(28b), which can be used to slow down the axial velocity of the atoms because the axial friction coefficient $\beta_{\rm axia}$ is larger than zero (i.e., the detuning from the resonant frequency $\Delta_1/(2\pi) = 0$ or $-\Delta_{\rm g}/(2\pi)$ is red one). From Eqs.(26) and (28b), for $I$=0.8mW/cm$^2$ and $\Delta_1 = -\Gamma$, we have also calculated the variation of the average axial dissipative force acting on the three-level $^{85}$Rb atoms with velocity $v_z$, and the result obtained is similar to that of the average azimuthal dissipative force, as shown in Fig.4. Therefore, the two counter-propagating HBBs with the same parameters can also be used to form 1D optical molasses and produce a pure damping force in the axial direction.

We also find that if the two-level atomic model is used to calculate the mean axial dissipative force on and its friction coefficient to a real alkali atom, the resulting errors are considerable.

## 3.3. The average dipole force

For a hyperfine three-level $^{85}$Rb atom in a linearly polarized HBB for $l$=1, $I$=0.8mW/cm$^2$, $\nabla I = 10^4$mW/cm$^3$ and $\nabla\Omega_1 = \nabla\Omega_2 = \sqrt{2}\Gamma\nabla I/\left(6\sqrt{I\,I_{\rm Sat}}\right)$, we have studied the variation of the average dipole forces acting on the three-level atoms with the detuning $\Delta_1/(2\pi)$ from Eq.(15) (see Fig.6). It is found that there are two pairs of the maximum absolute values of the average dipole force at the detuning $\Delta_1/(2\pi) = 0$ and $\Delta_1/(2\pi) = -\Delta_{\rm g}/(2\pi)$ for $\nabla\theta\,(\boldsymbol{R})\cdot\boldsymbol{v} = 0$, which shows a non-resonant property (with two pairs of "differential-curve" peaks) of the dipole force acting on the three-level atom and comes from two non-resonant effects between $|1\rangle \to |3\rangle$ and between $|2\rangle \to |3\rangle$. It can be seen from Fig.6 that the non-resonant property of the average dipole forces on a three-level atom is completely different from that on a two-level atom which has only a pair of non-resonant peaks at $\Delta_1/(2\pi) = 0$ or $\Delta_1/(2\pi) = -\Delta_{\rm g}/(2\pi)$. We also know from Fig.6 that the positions of the two peaks

will be shifted by $|\nabla\theta(\boldsymbol{R})\cdot\boldsymbol{v}|$ (the dashed line shown in Fig.6, $|\nabla\theta(\boldsymbol{R})\cdot\boldsymbol{v}| = 0.04$GHz, corresponding to $v_z$=30m/s) to the right for $\nabla\theta(\boldsymbol{R})\cdot\boldsymbol{v} > 0$ or to the left for $\nabla\theta(\boldsymbol{R})\cdot\boldsymbol{v} < 0$. Moreover, when the detuning is tuned away from the position of the maximum absolute value, the absolute value of the average dipole force will be decreased rapidly. We also find that the approximate expression of $\langle\boldsymbol{F}\rangle'_{\rm dipo}$ (see Eq.(20)), as shown by the dotted curve in Fig.6, will be equal to $\langle\boldsymbol{F}\rangle_{\rm dipo}$ given by Eq.(15) when the detuning from the maximum absolute-value peak is larger than $\sim$ 0.05GHz. In this case, the average dipole force expression $\langle\boldsymbol{F}\rangle_{\rm dipo}$ from the three-level atomic model can be approximated by the expression of $\langle\boldsymbol{F}\rangle'_{\rm dipo}$ from the two-level atomic model. Finally, Fig.6 shows that if the two-level atomic model is used to calculate the average dipole force on a real alkali atom in a HBB, the resulting error can reach 34%.

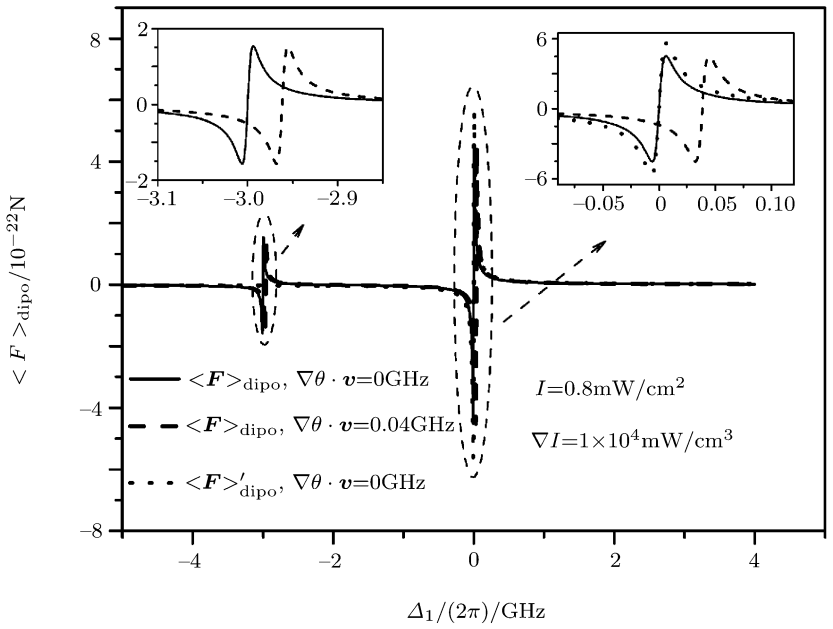



**Fig.6.** The variation of the average dipole force on the three-level atom (using Eq.(15) for $\nabla\theta(\boldsymbol{R})\cdot\boldsymbol{v}$=0GHz (solid line) and $\nabla\theta(\boldsymbol{R})\cdot\boldsymbol{v}$=0.04GHz (dashed line)) with $\Delta_1/(2\pi)$ for an $^{85}$Rb atom for $l$=1, $I$=0.8mW/cm$^2$, $\nabla I = 10^4$mW/cm$^3$, and the dotted line shows the average dipole force obtained using Eq.(20) for $\nabla\theta(\boldsymbol{R})\cdot\boldsymbol{v}$=0GHz.

The dependence of the average dipole force on the radial position $r$ of atomic motion in a HBB for $P$ = 10 mW, $k_r$=0.01$k_z$, $l$=1, and $\Delta_1/(2\pi)$=1GHz is also calculated, as shown in Fig.7. We find from Fig.7 that the intensity gradient is zero when $r$=0 or $r = r_0$ ($r_0$ is the position of the first maximum intensity of the HBB), and then the average dipole force is zero at the radial position of $r$=0 or $r = r_0$. So cold atoms moving into the region of $r < r_0$ in the blue-detuned HBB will be pushed to the minimum intensity position ($r$=0) of the HBB. This effect can be used to guide or trap cold atoms in the hollow region of the HBB. When the HBB is red-detuned, cold atoms will be attracted to the maximum-intensity ring of the HBB and trapped in a ring optical dipole well.

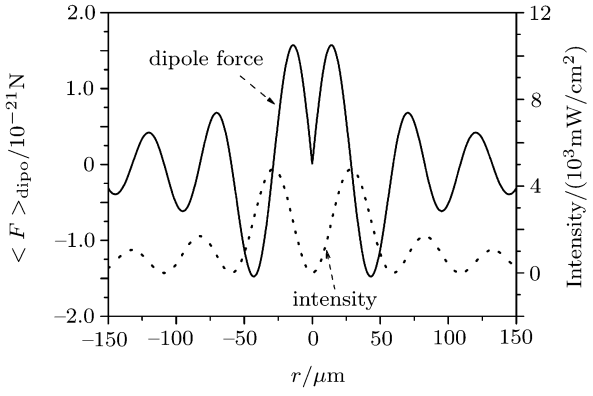



**Fig.7.** The variation of the average dipole force on the three-level atom with the radial position $r$ for an $^{85}$Rb atom for $P$ = 10 mW, $k_r$ = 0.01$k_z$, $l$=1, and $\Delta_1/(2\pi)$=1GHz.

# 4. Discussion and analysis

Each spontaneous emission accompanied by a momentum recoil $\hbar\boldsymbol{k}$ of the atom in a random direction may cause a diffusion of the atomic momentum (or result in heating), which can be characterized by a momentum diffusion coefficient $D$. In consideration of the photon absorption, the steady-state momentum diffusion coefficient $D$ may be approximately expressed as[21]

$$D = 2\hbar^2 k^2 \Gamma B, \tag{31}$$

where $B$ is the steady-state population in the upper level and given by Eq.(14). According to the Einstein relation $k_{\rm B}T = D/\beta$,[22] where $k_{\rm B}$ is the Boltzmann constant and $\beta$ the friction coefficient, we can obtain an approximate expression of the equilibrium temperature $T$ for the cooled atoms in 1D optical molasses formed by two counter-propagating red-detuning HBBs:

$$T = D/(k_{\rm B}\beta). \tag{32}$$

If we only consider the axial friction coefficient $\beta_{\rm axia}$, Eq.(32) can be rewritten as $T_{\rm axia} = D/(k_{\rm B}\beta_{\rm axia})$, by which we calculate the dependence of the axial temperature $T_{\rm axia}$ on the red detuning for $^{85}$Rb atoms at $I = 1.6\times10^{-4}{\rm mW/cm^2}$, and the result is shown by the solid line in Fig.8. We can find that there will be the minimum equilibrium temperature at $\Delta_1/(2\pi) \approx -6.0{\rm MHz}$ (i.e., $\Delta_1/(2\pi) \approx -\Gamma/(2\pi)$), and the minimum equilibrium temperature is about equal to the Doppler limit of $143.41\mu$K resulting from the two-level atomic model.[21] In the limit of the on-resonance saturation parameter (that is $s_0 = I/I_{\rm sat} \to 0$), in fact, we can obtain from Eq.(32) that the axial Doppler limit is $\hbar\Gamma/(2k_{\rm B})$, which is the same as the result from the two-level atomic model.[21] If the azimuthal friction effect is further considered, we can derive the equilibrium temperature of atoms in 1D molasses HBBs as follows:

$$T_{\rm all} = D/[k_{\rm B}\,(\beta_{\rm axia} + \beta_{\rm azim})]. \tag{33}$$

From Eq.(33), the corresponding Doppler cooling limit is given by

$$T_{\rm D} = \frac{\hbar\Gamma}{2k_{\rm B}} \cdot \frac{k^2}{k^2 + (l/r)^2}. \tag{34}$$

If we take $r = r_0 \approx 61.2\mu$m and $l = 4$,[6] the Doppler cooling limit is $143.40\mu$K. This shows that the azimuthal Doppler cooling can only be regarded as a supplement for the axial Doppler cooling in 1D molasses composed of a pair of usual HBBs, and the larger the orbital angular-momentum quantum number $l$ is (or the smaller the mean radius $r$ of atomic motion is), the more effective the Doppler cooling of atoms will be.

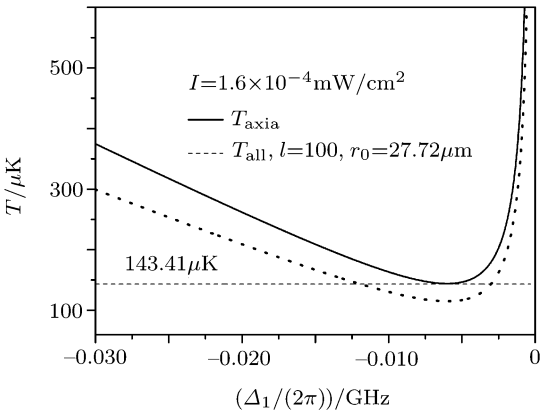



**Fig.8.** The dependence of the equilibrium temperature $T_{\rm axia}$ and $T_{\rm all}$ (with $l$=100 and $r_0 = 24.72\mu$m) on $\Delta_1/(2\pi)$ for a $^{85}$Rb atom for a small light intensity $I = 1.6\times10^{-4}{\rm mW/cm^2}$.

For the $l$th-order Bessel beam, the first maximum-intensity radius $r_0$ of the HBB is increased with the increase of $l$. Generally, $k_r r \ll 1$ in Eq.(21) ( here $k_r$ is the radial component of the wavevector $k$), we can obtain the approximate relationship between the radius $r_0$ of the first maximum intensity and $l$ as follows:

$$r_0 = \frac{2}{k_r}\sqrt{\frac{l\,(l+1)}{l+2}}. \tag{35}$$

We know from Eq.(35) that the increase of $r_0$ is faster than that of $l$, so the Doppler cooling limit given by Eq.(34) can be effectively lowered by increasing the orbital angular-momentum quantum number $l$ of the HBB. For example, when $l$=100,[23] we obtain $r_0 = 247.19\mu$m and $T_{\rm D} = 143.05\mu$K as $k_r = 0.01k$ from Eqs.(34) and (35). In particular, if a pair of reduced HBBs with an orbital angular-momentum quantum number of $l$=100 and a magnification of $M = 1/10$ (i.e., $r_0 = 24.72\mu$m) as $k_r = 0.01k$ is used to form 1D molasses, the variation of the equilibrium temperature $T_{\rm all}$ of atoms in 1D molasses HBBs with the red detuning for $^{85}$Rb atoms as $I = 1.6\times10^{-4}{\rm mW/cm^2}$ is expressed as the dashed line in Fig.8. We can find that the Doppler cooling limit is $T_{\rm D} = 114.5\mu$K, which is far lower than the conventional Doppler cooling limit ($143.41\mu$K) for $^{85}$Rb atoms.

## 5. Conclusion

We have derived the general expressions of the average dissipative and dipole forces acting on a Λ-configuration three-level atom in a light field, and found a resonant property (with two resonant peaks) of the dissipative force and a non-resonant property (with two pairs of non-resonant peaks) of the dipole force on the three-level atom. Both expressions of the average dissipative and dipole forces on the three-level atom can be simplified to those on a two-level atom under the approximation of large detuning. Furthermore, we have analysed the general properties of the average dissipative force on the three-level atom in the linearly-polarized HBB and find a saturation effect of the average dissipative force.

Our study has shown that: (1) If the two-level atomic model is used to calculate the mean azimuthal dissipative force at the resonant position $\Delta_1/(2\pi) = 0$, the resulting errors of the maximum azimuthal dissipative force and its FWHM will be 47% and 25%, respectively. And if the two-level atomic model is used to calculate the azimuthal friction coefficient for a real alkali atom, the resulting error is also considerable. (2) If the two-level atomic model is used to calculate the average axial dissipative force and its friction coefficient as well as the average dipole force for a real alkali atom, the resulting errors are considerable. (3) Two counter-propagating HBBs with an orbital angular-momentum quantum number of $l_1 = l_2 = l$ and a red detuning can be used to form 1D optical molasses in both the axial and azimuthal directions and produce a pure damping force for the trapped atoms in the small velocity regime. We have also discussed the azimuthal effect on Doppler limit, and found that the azimuthal Doppler cooling effect can be regarded as a supplement for the axial Doppler cooling, and the larger the orbital angular-momentum quantum number $l$ is, the lower the Doppler cooling limit of atoms will be. In particular, when $l = 100$, $r_0 = 24.72\mu$m and $k_r = 0.01k$, we obtain $T_{\rm D} = 114.5\mu$K, which is far lower than the conventional Doppler cooling limit ($T_{\rm D} = 143.41\mu$K) of $^{85}$Rb atoms. To our knowledge, this is a new discovered effect in Doppler laser cooling of neutral atoms.

From the important results mentioned above, we conclude that the theory of Doppler laser cooling based on a two-level atomic model[10,16] would result in considerable error for a real alkali atom, and we should take three-level atomic model to deal with problems in Doppler laser cooling and consider the azimuthal effect on Doppler limit for large quantum number of orbital angular-momentum.

## References


[1] Yin J, Gao W and Zhu Y 2003 *Prog. Opt.* **45** 119
[2] Durmin J, Miceli J J and Eberly J H 1987 *Phys. Rev. Lett.* **58** 1449
[3] Herman R M and Wiggins T A 1991 *J. Opt. Soc.Am.* A **8** 932
[4] Lee H S, Stewart B W, Choi K and Fenichel H 1994 *Phys. Rev.* A **49** 4922
[5] Paterson C and Smith R 1996 *Opt. Commun.* **124** 121
[6] Arlt J and Dholakia K 2000 *Opt. Commun.* **177** 297
[7] Allen L, Babiker M and Power W L 1994 *Opt. Commun.* **112** 141
[8] Power W L, Allen L, Babiker M and Lembessis V E 1995 *Phys. Rev.* A **52** 479
[9] Allen L, Babiker M, Lai W K and Lembessis V E 1996 *Phys. Rev.* A **54** 4259
[10] Babiker M, Lembessis V E, Lai W K and Allen L 1996 *Opt. Commun.* **123** 523
[11] Lai W K, Babiker M and Allen L 1997 *Opt. Commun.* **133** 487
[12] Babiker M, Power W L and Allen L 1994 *Phys. Rev. Lett.* **73** 1239
[13] Lembessis V E 1999 *Opt. Commun.* **159** 243
[14] Tan L, Wang Z C and Gu H Q 2004 *Chin. Phys.* **13** 1005
[15] Hu Z F, Du C G and Li S Q 2003 *Chin. Phys.* **12** 403
[16] Hansch T W and Schawlow A L 1975 *Opt. Commun.* **13** 68
[17] Harris S E 1997 *Phys. Today* **50** 36
[18] Marangos J P 1998 *J. Mod. Opt.* **45** 471
[19] Javanainen J 1992 *Europhys. Lett.* **17** 407
[20] Wang Z and Yin J 2006 *Phys. Rev.* A **74** 013408
[21] Meystre P 2001 *Atom Optics* (New York: Springer)
[22] Grynberg G. and Robilliard C 2001 *Phys. Rep.* **355** 335
[23] Courtial J, Dholakia K, Allen L and Padgett M J 1997 *Opt. Commun.* **144** 210